MAGNETISM

I – FUNDAMENTALS

edited by

Étienne du TRÉMOLET de LACHEISSERIE
Damien GIGNOUX
Michel SCHLENKER

Grenoble Sciences

2002

AUTHORS

Michel CYROT - Professor at the Joseph Fourier University of Grenoble, France

Michel DÉCORPS - Senior Researcher, INSERM (French Institute of Health and Medical Research), Bioclinical Magnetic Nuclear Resonance Unit, Grenoble

Bernard DIÉNY - Researcher and group leader at the CEA (French Atomic Energy Center), Grenoble

Etienne du TRÉMOLET de LACHEISSERIE - Senior Researcher, CNRS, Laboratoire Louis Néel, Grenoble

Olivier GEOFFROY - Assistant Professor at the Joseph Fourier University of Grenoble

Damien GIGNOUX - Professor at the Joseph Fourier University of Grenoble

Ian HEDLEY - Researcher at the University of Geneva, Switzerland

Claudine LACROIX - Senior Researcher, CNRS, Laboratoire Louis Néel, Grenoble

Jean LAFOREST - Research Engineer, CNRS, Laboratoire Louis Néel, Grenoble

Philippe LETHUILLIER - Engineer at the Joseph Fourier University of Grenoble

Pierre MOLHO - Researcher, CNRS, Laboratoire Louis Néel, Grenoble

Jean-Claude PEUZIN - Senior Researcher, CNRS, Laboratoire Louis Néel, Grenoble

Jacques PIERRE - Senior Researcher, CNRS, Laboratoire Louis Néel, Grenoble

Jean-Louis PORTESEIL - Professor at the Joseph Fourier University of Grenoble

Pierre ROCHETTE - Professor at the University of Aix-Marseille 3, France

Michel-François ROSSIGNOL - Professor at the Institut National Polytechnique de Grenoble (Technical University)

Yves SAMSON - Researcher and group leader at the CEA (French Atomic Energy Center) in Grenoble

Michel SCHLENKER - Professor at the Institut National Polytechnique de Grenoble (Technical University)

Christoph SEGEBARTH - Senior Researcher, INSERM (French Institute of Health and Medical Research), Bioclinical Magnetic Nuclear Resonance Unit, Grenoble

Yves SOUCHE - Research Engineer, CNRS, Laboratoire Louis Néel, Grenoble

Jean-Paul YONNET - Senior Researcher, CNRS, Electrical Engineering Laboratory, Institut National Polytechnique de Grenoble (Technical University)

Grenoble Sciences

"Grenoble Sciences" was created ten years ago by the Joseph Fourier University of Grenoble, France (Science, Technology and Medicine) to select and publish original projects. Anonymous referees choose the best projects and then a Reading Committee interacts with the authors as long as necessary to improve the quality of the manuscript.

(Contact : Tél. : (33)4 76 51 46 95 - E-mail : Grenoble.Sciences@ujf-grenoble.fr)

The "Magnetism" Reading Committee included the following members :

- **V. Archambault**, Engineer - Rhodia-Recherche, Aubervilliers, France
- **E. Burzo**, Professor at the University of Cluj, Rumania
- **I. Campbell**, Senoir Researcher - CNRS, Orsay, France
- **F. Claeyssen**, Engineer - CEDRAT, Grenoble, France
- **G. Couderchon**, Engineer - Imphy Ugine Précision, Imphy, France
- **J.M.D. Coey**, Professor - Trinity College, Dublin, Ireland
- **A. Fert**, Professor - INSA, Toulouse, France
- **D. Givord**, Senior Researcher - Laboratoire Louis Néel, Grenoble, France
- **L. Néel**, Professor, Nobel Laureate in Physics, Member of the French Academy of Science
- **B. Raquet**, Assistant Professor - INSA, Toulouse, France
- **A. Rudi**, Engineer - ECIA, Audincourt, France
- **Ph. Tenaud**, Engineer - UGIMAG, St-Pierre d'Allevard, France

"Magnetism" (2 volumes) is an improved version of the French book published by "Grenoble Sciences" in partnership with EDP Sciences with support from the French Ministry of Higher Education and Research and the "Région Rhône-Alpes".

EXTRAITS

Thus man works with magnetic field intensities spanning a scale of 17 decades (fig. 1.6); for reference, the earth's magnetic field is of the order of a few tens of amperes per meter.

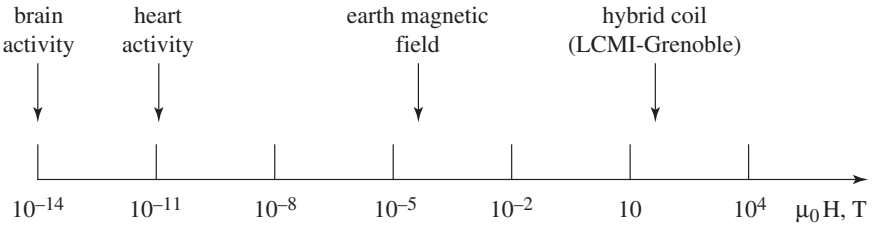

Figure 1.6 - Range of experimentally accessible magnetic fields

Permanent magnets

Our grandmothers used only horse-shoe shaped magnets to collect their sewing needles, as magnets of the day had a tendency to spontaneously demagnetise, and this specific shape led to maximum "flux line" closure, and thus minimised the risk of demagnetization (see fig. 1.2).

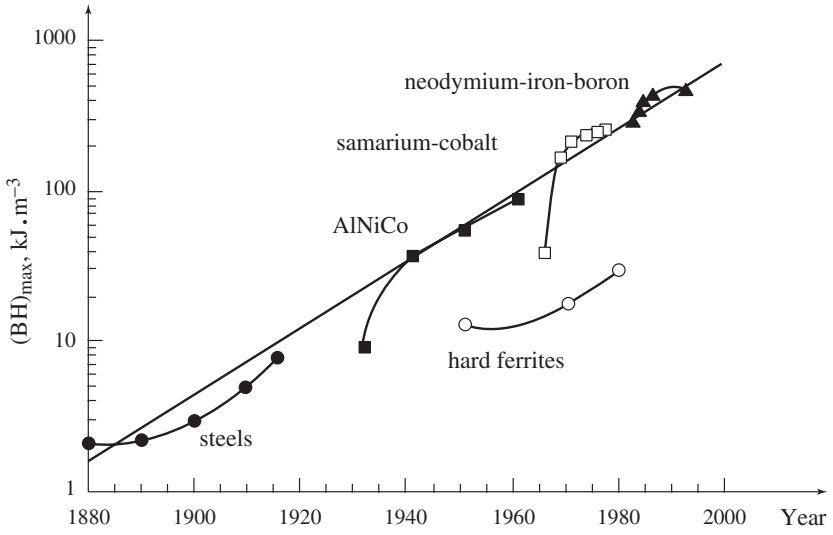

Figure 1.7 - Evolution in the performance of permanent magnets as characterised by their energy products

Logarithm of the maximum energy product ($[BH]_{max}$) expressed in $kJ.m^{-3}$ and plotted as a function of the date of their arrival on the permanent magnet market for different materials belonging to the five principal industrial magnet families, after [11]. The concept of induction, magnetic field and energy product will be discussed in the following chapter.

Today's Nd-Fe-B magnets can remain magnetised in thin sheet form, even when magnetised perpendicular to the plane of the sheet. The progress made over 150 years

1.2.2. The determination of B (and A) from bound currents: the Ampérian approach

In the presence of matter, one can show (see appendix § 3 at the end of this chapter) that the determination of the induction **B** and the vector potential **A** at all points in space can be reduced to a problem of electromagnetism in vacuum where two types of current have to be considered:

- on the one hand the real *free currents* with density $\mathbf{j}_0$, and
- on the other hand the currents associated with the magnetised material, or bound currents, with volume and surface densities, $\mathbf{j}_m$ and $\mathbf{j}_{ms}$ respectively, given by:

$$\mathbf{j}_m = \mathbf{curl}\,\mathbf{M} \tag{2.32}$$

$$\mathbf{j}_{ms} = \mathbf{M} \times \hat{\mathbf{n}} \tag{2.33}$$

where $\hat{\mathbf{n}}$ is the unit vector normal to the surface of the material, and pointing outwards. equation (2.32) reduces to (2.33) when one only considers the surface as the transition between the material ($\mathbf{M} \neq 0$ inside) and the vacuum ($\mathbf{M} = 0$ outside), and going to the limit where δ (the thickness) goes to zero. One can thus determine **B** using the method given in section 1.1.3 taking $\mathbf{j} = \mathbf{j}_0 + \mathbf{j}_m$.

Notes

- *When the magnetization is uniform, which is often the case, $\boldsymbol{j}_m = 0$, and only the surface current density $\boldsymbol{j}_{ms}$ is left. An example, the **B** field produced everywhere (inside and outside of the cylinder) by a cylinder uniformly magnetised along its cylindrical axis is the same as from a solenoid of current density (current per unit length along the solenoid) $|\boldsymbol{j}_{ms}| = |\boldsymbol{M}|$ (see fig. 2.9).*
- *The conditions at the interface between two materials are the same as those given in section 1.1.4, taking into account the fact that **i** (or rather $\boldsymbol{i}_s$ in eq. 2.15) is the sum of the free and bound current densities.*
- *One can always write that:*

$$\boldsymbol{B} = \boldsymbol{B'}_0 + \boldsymbol{B}_m \tag{2.34}$$

where $\boldsymbol{B'}_0$ and $\boldsymbol{B}_m$ are the contributions from the free currents and magnetised material respectively.

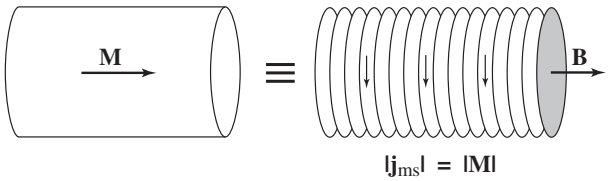

Figure 2.9 - The equivalence between magnetization and surface current density in the case of a cylinder uniformly magnetised parallel to its cylindrical axis

Along <100>, magnetization is the highest, and it reaches its maximum value in very low field; it is the easy magnetization direction. In zero field, the material is divided into six types of domains, called *phases*, in which the spontaneous magnetization $\mathbf{M}_s$ is directed along one of these directions. When the field is applied along the <110> and <111> axes, the *phase rule* is observed: in very weak field the magnetization remains parallel to <100>, and the magnetizations extrapolated to zero internal field, $M_{<110>}$ and $M_{<111>}$ (fig. 3.15), correspond to the projection of the spontaneous magnetization $M_{<100>} = M_s$ along each of these directions ($M_{<110>} = M_s / \sqrt{2}$, and $M_{<111>} = M_s / \sqrt{3}$).

An analysis similar to that previously developed in the uniaxial situation shows that:

- the area between the curves measured as a function of the internal field H along the <100> and <110> directions is equal to $K_1 / 4$,
- and the field for which these two curves meet can be written as $H_{A<110>} = 2K_1 / \mu_0 M_s$.

2.4.3. Magnetic anisotropy in the paramagnetic state

Let us note that in uniaxial systems, of hexagonal or tetragonal symmetry for instance, in which magnetism originates from rare earth atoms having $L \neq 0$ (see chap. 7), the strong magnetocrystalline anisotropy of the latter leads to an *anisotropy of the magnetic susceptibility*. In particular, above the ordering temperature, two shifted Curie-Weiss laws are observed for the susceptibilities parallel and perpendicular to the high symmetry **c** axis, namely:
$1 / \chi_{\parallel} = (T - \theta_{p\parallel}) / \mathscr{C}$ and $1 / \chi_{\perp} = (T - \theta_{p\perp}) / \mathscr{C}$. In this case the difference between the parallel ($\theta_{p\parallel}$) and perpendicular ($\theta_{p\perp}$) paramagnetic Curie temperatures is a measure of the main contribution to the anisotropy, namely the second order term.

2.5. TIME DEPENDENT PHENOMENA

Once a magnetic field is applied on a ferromagnetic substance, the magnetization of the latter reaches a value which depends on the intensity of the magnetic field, on the nature of the substance, on the temperature, but also on the history of the considered sample: in particular, magnetization often strongly depends on the order in which *thermal treatments*, *mechanical stresses*, and variations of the *magnetic field* have been made. However another key parameter has also to be considered, namely *time*, because time dependence of magnetic properties is often observed: *a substance submitted to a magnetic field does not immediately reach a final and well defined magnetization*.

Many effects contribute to this time dependence of magnetization:

- *aging* means an evolution of magnetic properties associated with irreversible modifications of the structure of the material under investigation (for instance, formation of precipitates); these structural modifications result from mechanical treatments, chemical effects (oxidation or others) or from atomic diffusion phenomena.

- various *relaxation* phenomena can also be observed. We will see in section 2 of chapter 4 that a certain time interval, which can reach 10^{-12} to 10^{-7} s, elapses before an *atomic magnetic moment* becomes parallel to the field which has just been applied; this relaxation phenomenon can be critical in some applications in fast electronics (see chap. 17 and 23). At the scale of the sample, a relaxation of electromagnetic origin can also be observed in conductors. It is due to *eddy currents,* associated with magnetic flux variations in the material which, during some seconds or fractions of a second, oppose the penetration of a rapidly changing field into the metallic material. The speed of the domain wall motion, measured by Sixtus and Tonks inside metallic fibres [5], is –for instance– in agreement with what is predicted by calculations which account for the delay imposed by the eddy currents.
- *magnetic after-effect*: once a magnetic field has been applied, magnetization changes only after a certain time, and goes on changing during a time range which allows experiments; there is a delay between the cause and its effect. One distinguishes the thermal fluctuation after-effect (irreversible), of thermodynamic character, and occurring in all ferromagnetic substances, and the diffusion after-effect (reversible) due to motion of particles inside the material. Two major works [6, 7] give an excellent and detailed presentation of these effects, which are briefly presented hereafter, and which are developed in section 5 of chapter 6.

2.5.1. Thermal fluctuation after-effect

We have seen in figure 3.5 that, for the same value of the magnetic field, three different values of magnetization could be obtained: the first corresponds to the initial magnetization curve, the second is observed when the magnetic field decreases from a high and positive value, and the third when the field increases from negative values. Each of these values corresponds to a minimum of the total energy of the system, but they are metastable equilibria. In particular it is the case of the remanent magnetization, that is observed when the magnetic field is reduced down to zero after saturation of the sample. One easily imagines that thermal agitation allows the system to slowly evolve toward a more stable equilibrium state: the remanent magnetization then decreases little by little, and tends more and more slowly toward zero, a value reached for an infinite time. The final equilibrium state ($M = 0$, $H = 0$) will be the same whatever the sign and the intensity of the magnetic field applied before it is reduced to zero.

This point ($M = 0$, $H = 0$) corresponds to the origin of the so called *anhysteretic magnetization curve* of the substance. As a matter of fact, to any non zero value H_0 of the magnetic field applied to a ferromagnetic substance, there also corresponds a unique value of the anhysteretic magnetization, the value which would be observed for an infinite time. However there is a more realistic technique to obtain this anhysteretic magnetization curve for a soft material. It consists in superposing to the static field H_0 an AC magnetic field which is slowly decreased down to zero: the final

value is the required magnetization. Figure 3.16 shows the result obtained in this way on an alloy of iron with a small amount of silicon: the anhysteretic curve has been plotted in the first quadrant ($H > 0$, $M > 0$). It lies above any experimental curve strarting from the origin (the initial magnetization curve included), and below any curve measured in decreasing field from a field larger than the saturation field.

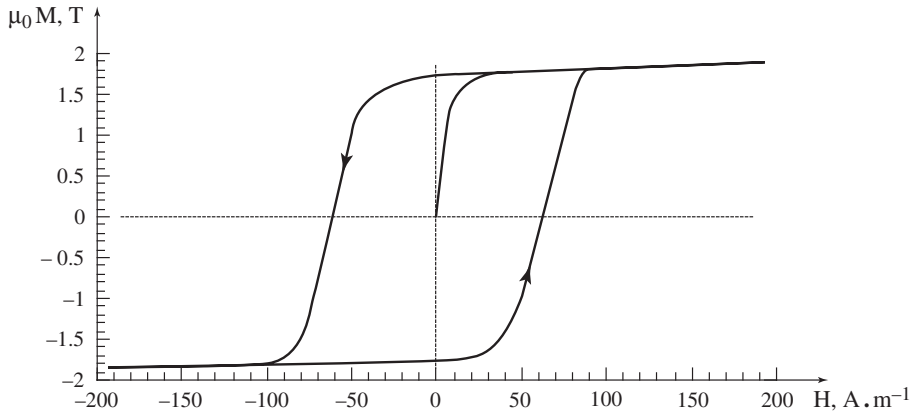

Figure 3.16 - Magnetization curve of a textured Fe-Si alloy: hysteresis loop and anhysteretic curve

The purely magnetic after-effect that has just been discussed only implies magnetic moment reversal. The host crystal or amorphous material is assumed to be perfectly stable: the values of the saturation magnetization and of the magnetocrystalline anisotropy constants remain constant in this process.

2.5.2. Diffusion after-effect

Contrary to the previous situation, diffusion after-effect is associated with the reversible diffusion of atoms, and / or of vacancies between interstitial lattice sites of the magnetic material. This can lead to a variation of its magnetization, and even of its anisotropy constants: the main magnetic characteristics of the substance are then modified. This effect takes place only in substances that can contain small size impurities in interstitial sites (carbon, nitrogen, ...), and it only occurs in the temperature range where diffusion of these impurities is fast enough. It can be used to induce, in an initially isotropic material, a uniaxial magnetic anisotropy called *induced anisotropy*. In this way, for instance, ferrite manufacturers can optimise the performance of their products.

3. PHYSICAL PHENOMENA ASSOCIATED WITH MAGNETISM

So far we have considered the effects of an applied magnetic field on the magnetic response, i.e. magnetization or magnetic induction. In fact magnetism in a substance also gives rise to secondary effects, which affect all physical properties: thermal,

For the sake of simplicity, one only considers, which is reasonable, the interactions between moments of the same layer, and between those belonging to first and second nearest neighbour layers. Let w_0, w_1 and w_2 be the molecular field coefficients due to the moments of the same layer, and to those of first and second neighbour layers, respectively. The exchange energy density is then written as:

$$E_{ex} = -\mu_0 M_c^2 (w_0 + 2 w_1 \cos\phi + 2 w_2 \cos 2\phi) / 2 \qquad (4.64)$$

Minimizing this energy with respect to ϕ leads to the equation $(w_1 + 4w_2 \cos\phi) \sin\phi = 0$, which is satisfied for three magnetic configurations:

- $\phi = 0$, i.e. ferromagnetism,
- $\phi = 180°$, i.e. antiferromagnetism,
- an angle ϕ given by:

$$\cos\phi = -w_1 / 4w_2 \qquad (4.65)$$

This latter case corresponds to helimagnetism. It is sketched in figure 4.19-a.

Let us notice that this configuration can exist only if $|w_1 / 4w_2| < 1$. Furthermore, the study of the sign of the second derivative of the energy, and comparison of the energies of these configurations, leads to the phase diagram shown in figure 4.20. The helimagnetic configuration is the most stable when $w_2 < 0$ and $|w_2| > |w_1 / 4|$. Such a structure is observed in a large number of hexagonal, and to a lesser extent tetragonal rare earth based compounds.

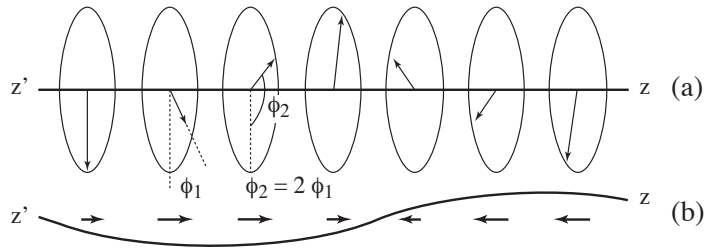

Figure 4.19 - Helimagnetic (a), and sine wave modulated structures (b)

7.2. SINE WAVE MODULATED STRUCTURE

Let us now consider the case where the uniaxial anisotropy forces the moments to be along the z axis, i.e. perpendicular to the layers. The only degree of freedom left to magnetization is then its amplitude: let us assume that it exhibits a sine wave modulation (fig. 4.19-b) with: $M_n = M_{max} \cos(n\phi + \phi_0)$, where n = … –2, –1, 0, 1, 2, … numbers the successive layers.

Considering the same exchange interactions as previously, the energy density is written as:

$$E_{ex} = (\mu_0 / 2)(M_{max})^2 \cos\phi_0 \{ w_0 \cos\phi_0 + w_1 [\cos(\phi + \phi_0) + \cos(-\phi + \phi_0)] + w_2 [\cos(2\phi + \phi_0) + \cos(-2\phi + \phi_0)] \}$$

solution to the equation). Figure 5.11 shows the evolution of the reduced thickness $\delta / a = N$ (number of interatomic intervals in the wall) as a function of the ratio η of the anisotropy and exchange constants of the material.

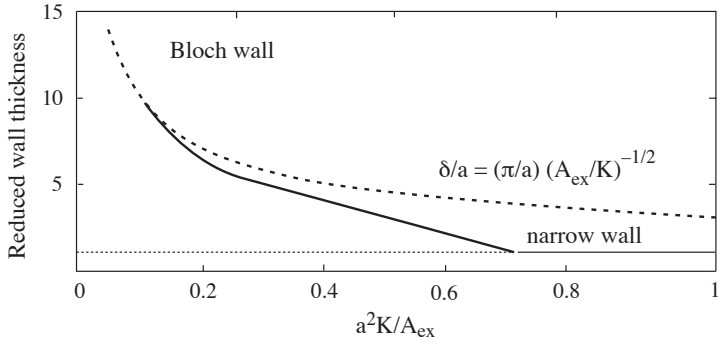

Figure 5.11 - Wall thickness as a function of η

The reduced thickness of the domain wall is expressed in units of interatomic distances.

3.3. DOMAIN WALLS IN VERY THIN FILMS

In thin film systems, the demagnetising fields are very important in the direction corresponding to the small dimension, this is why the magnetization in the domains generally orients itself in the plane of the film. Let us consider two adjacent domains separated by a 180° wall. A Bloch wall, where moments rotate about the normal to the surface of the wall (see fig. 5.12-a), leads to the appearance of magnetic poles which are north on one face of the thin film and south on the other. The associated magnetostatic energy becomes greater as the ratio of the thickness of the film (e) over the width of the domain wall (δ) is reduced. Taking this magnetostatic energy into account leads to a new expression for the the domain wall energy:

$$\gamma = \frac{1}{2}\gamma_0\left(\frac{\delta}{\delta_0} + \frac{\delta_0}{\delta} + \frac{\mu_0 M_s^{\,2}}{2\gamma_0}\frac{\delta^2}{e}\right),$$

where γ_0 and δ_0 are, respectively, the energy, and thickness of the ordinary Bloch wall. This approximation is valid as long as δ remains small compared to e. This domain wall energy is thus the sum of three contributions, respectively magneto-crystalline anisotropy which varies as δ, exchange energy which varies as δ^{-1}, and dipolar energy which varies as δ^2.

γ is not only a function of the properties of the material, but also of the thickness of the film. For small thicknesses other domain wall structures are favoured. Néel considered in particular [5] a domain wall structure in which the moments rotate about the axis perpendicular to the plane of the film (fig. 5.12-b). The contribution of the magnetic poles is eliminated, but the configuration of the moments inside the wall leads to stray field.

A 180° wall, assumed to be plane, rigid and parallel to one of the faces of the cube of defects, has a surface energy γ. When the position of the wall coincides with any one of the lattice planes of defects, its surface area is minimal because the surface of the holes produced by the defects inside the wall is maximal. Per unit area of the wall, there are $1/a^2$ holes, each with an area $\mathcal{A} = \pi r^2$. Thus these lattice planes are energy minima where, in the absence of a field, the wall is in equilibrium. When displaced from one of these equilibrium positions by an amount x less than r, the wall area is now decreased by the defects by only an area $\mathcal{A}'$. The relative variation of the area is $\delta\mathcal{A}/a^2 = (\mathcal{A} - \mathcal{A}')/a^2 = \pi (r^2 - x^2)/a^2$.

The change in energy of a wall in the neighbourhood of the lattice planes is then given by:

$$\Delta E_p(x) = \pi x^2 \gamma / a^2 \tag{6.13}$$

which, for a magnetic system of unit surface area containing only one wall (fig. 6.8-a), leads to an energy profile schematised in figure 6.8-b. A restoring force in the direction of the equilibrium position exists only within the zone of width r on either side of each of the minima (fig. 6.8-c). Its value is:

$$F_r = -dE_p/dx = -2 \pi x \gamma \tag{6.14}$$

Decrease of magnetostatic energy associated with the presence of a defect

Although it is not negligible, the role of the demagnetising field in the neighbourhood of non-magnetic defects was completely ignored in the preceding model. The magnetostatic energy associated with a non-magnetic spherical void or inclusion with radius r, completely immersed in a magnetic domain (fig. 6.9-a), is given by:

$$E_{d_0} = \frac{2}{9} \mu_0 \pi M_s{}^2 r^3 \tag{6.15}$$

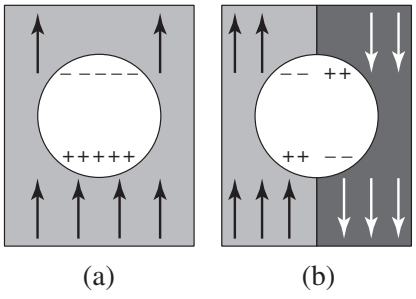

Figure 6.9 - The strong magnetostatic energy linked to the state (a) of a spherical inclusion placed in a medium with uniform magnetization is reduced if the wall crosses this spherical inclusion (b)

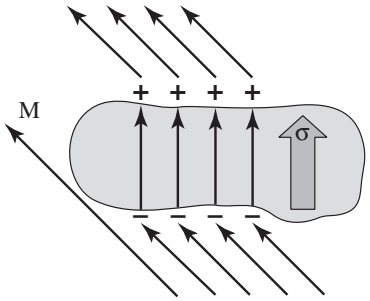

Figure 6.10 - The stress σ causes the moments to deviate locally, and thus creates regions where magnetic masses appear

where λ is negative for a shell less than half full, and positive for the opposite case, so that the spin and orbital moments prefer to be anti-parallel and parallel respectively. In particular λ is negative in the case of a single electron [2].

1.2.4. Multiplets

The degeneracy of each term is partially lifted by the spin-orbit interaction outlined above. Each new energy level, known as a "*multiplet*", is characterised by an integer or half integer quantum number J which in turn characterises the total angular momentum $\hbar\mathbf{J}$ such that:

$$\mathbf{J} = \mathbf{L} + \mathbf{S} \tag{7.21}$$

Within a multiplet, there exists a basis of $2J + 1$ states $|\, L, S, J, M_J \rangle$ such that M_J can take the values + J to – J in steps of one. They are the eigen states of $\mathbf{J}^2$ and J_z such that:

$$\mathbf{J}^2 |\, L, S, J, M_J \rangle = J(J + 1) |\, L, S, J, M_J \rangle \tag{7.22}$$

and

$$J_z |\, L, S, J, M_J \rangle = M_J |\, L, S, J, M_J \rangle \tag{7.23}$$

Each multiplet is thus $2J + 1$ times degenerate. The values of J of the different multiplets arising from the same term vary from $L + S$ to $|L - S|$ in steps of one. By squaring equation (7.21) it can be deduced that $\mathcal{H}_{so} = -(\lambda/2)(\mathbf{J}^2 - \mathbf{L}^2 - \mathbf{S}^2)$. The energy of a multiplet is thus given by:

$$E_J = \langle \mathcal{H}_{so} \rangle = -(\lambda/2)\,[J(J + 1) - L(L + 1) - S(S + 1)].$$

The ground state multiplet is such that $J = L + S$ if the shell is more than half full, and $J = |L - S|$ when it is less than half full. If the shell is exactly half full, J = S as Hund's rules give L = 0. The spin-orbit coupling increases with the atomic number of the element under consideration. The difference between two multiplets is typically of the order of 10^{-2} to 10^{-1} eV (10^2 to 10^3 K) for elements in the iron group, and 1 eV (10^4 K) for the rare earths. The schematic diagram in figure 7.7 shows, for the case of the Cr^{3+} ion, the different stages leading to the ground state energy of a free atom (or ion).

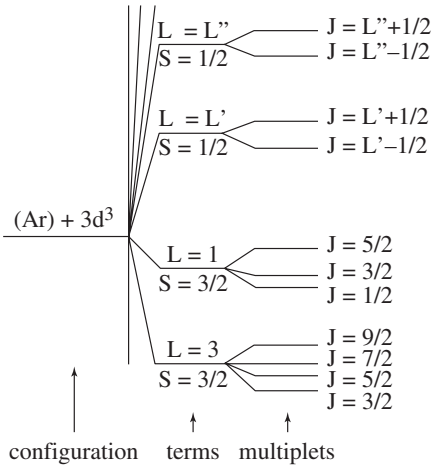

Figure 7.7 - Splitting of the ground state configuration of the Cr^{3+} ion into its terms, and multiplets

At this stage, the further liftings of the degeneracy can only take place as a result of external perturbations such as a magnetic field (Zeeman effect), or the effects of neighbouring atoms when the atom is no longer free, and is part of a solid. The multiplets are generally referred to by symbols such as $^2S_{1/2}$, $^3P_0$, $^4F_{9/2}$, etc. This is the *spectroscopic notation* where the letters S, P, D, F, G, H, I, … refer to the total orbital angular momentum L = 0, 1, 2, 3, 4, 5, 6, … respectively. The numbers at the top left, and bottom right are 2S + 1, and J respectively.

As a result of the energy differences between the different multiplets, one can neglect the effect of all but the lowest lying multiplet when considering the rare earth elements (4f series). At normal temperatures the occupation of the higher multiplets is negligible.

In addition to the electronic structure of the free atom, the periodic table in appendix 3 also gives the spectroscopic ground states. It can be seen from table 3.1 that all non magnetic free atoms in their ground state are characterised by J = 0 (spectroscopic levels $^1S_0$, $^3P_0$, $^5D_0$, etc.). It will be shown in what follows that the magnetic moment of an atom or ion is strictly linked to its quantum number J.

Consider the magnetic moment associated with the orbital angular momentum of a multiplet. Using equation (7.6), the orbital magnetic moment is written as:

$$\mathfrak{m}_o = -\mu_B \mathbf{L} \tag{7.24}$$

Similarly, using equation (7.9), the spin magnetic moment is written as:

$$\mathfrak{m}_S = -2\mu_B \mathbf{S} \tag{7.25}$$

As has been already mentioned, equations (7.24), and (7.25) show that the total magnetic moment $\mathfrak{m} = \mathfrak{m}_0 + \mathfrak{m}_S$ has no constraint that forces it to be collinear with the total angular momentum $\hbar\mathbf{J} = \hbar(\mathbf{L} + \mathbf{S})$. In fact, quantum mechanics reveals that *within each multiplet* the total magnetic moment and the total angular momentum can be considered to be collinear, and linked by the formula:

$$\mathfrak{m} = -g_J \mu_B \mathbf{J} \tag{7.26}$$

where g_J, the *Landé g factor*, characterises the multiplet under consideration. It is expressed as a function of J, L, and S such that:

$$g_J = 1 + \frac{J(J+1) + S(S+1) - L(L+1)}{2J(J+1)} \tag{7.27}$$

g_J is 1 or 2 when only the orbital or spin contributions are present respectively, but is not forced to lie within these values. As an example one can see from table 7.1 that g_J is less than one when L > S, and when J = L – S.

The main magnetic properties of R^{3+} ions in the rare earth series are given in table 7.1. It is in this valence state that these elements are found in most materials. Note however that cerium can also be tetravalent, and samarium, europium, and ytterbium can be divalent.

Note - *The above result has been established for the almost ideal case of isolated atoms. It will become apparent in what follows that it holds for substances where the magnetic atom is not too perturbed by interatomic interactions. Irrespective of the substance under consideration, it is always possible to write that the magnetic moment* $\mathcal{m}$ *and the angular momentum* $\mathcal{L}$ *of the atoms are proportional:*

$$\mathcal{m} = -g\frac{e}{2m_e}\mathcal{L} = \gamma\mathcal{L} \qquad (7.28)$$

γ *is the gyromagnetic factor. Its value allows the estimation of the relative size of the orbital and spin contributions (*$\gamma = -(e/2m_e)$ *and* $\gamma = -2\,(e/2m_e)$ *respectively) to the magnetic moment in a given substance.*

Points to remember:

- Filled electronic shells are not magnetic.
- Only non saturated shells have a magnetic moment.
- The magnetic moment of free atoms or ions is given by: $\mathcal{m} = -g_J \mu_B \mathbf{J}$ where $\hbar\mathbf{J}$ is the total angular momentum. For a given configuration, the quantum number J, and thus g_J, are determined by Hund's rules.

Table 7.1 - The main properties of free R^{3+} ions of the elements in the rare earth or lanthanide group R

Ion 4f	$^{2S+1}L_J$	L	S	J	gJ	$\mathcal{m}_0$ (μ_B)	$\mathcal{m}_{eff}$ (μ_B)
Ce^{3+} ($4f^1$)	$^2F_{5/2}$	3	1/2	5/2	6/7	2.14	2.54
Pr^{3+} ($4f^2$)	$^3H_4$	5	1	4	4/5	3.20	3.58
Nd^{3+} ($4f^3$)	$^4I_{9/2}$	6	3/2	9/2	8/11	3.27	3.62
Pm^{3+} ($4f^4$)	$^5I_4$	6	2	4	3/5	2.40	2.68
Sm^{3+} ($4f^5$)	$^6H_{5/2}$	5	5/2	5/2	2/7	0.71	0.85
Eu^{3+} ($4f^6$)	$^7F_0$	3	3	0	–	0	0
Gd^{3+} ($4f^7$)	$^8S_{7/2}$	0	7/2	7/2	2	7.00	7.94
Tb^{3+} ($4f^8$)	$^7F_6$	3	3	6	3/2	9.00	9.72
Dy^{3+} ($4f^9$)	$^6H_{15/2}$	5	5/2	15/2	4/3	10.00	10.65
Ho^{3+} ($4f^{10}$)	$^5I_8$	6	2	8	5/4	10.00	10.61
Er^{3+} ($4f^{11}$)	$^4I_{15/2}$	6	3/2	15/2	6/5	9.00	9.58
Tm^{3+} ($4f^{12}$)	$^3H_6$	5	1	6	7/6	7.00	7.56
Yb^{3+} ($4f^{13}$)	$^2F_{7/2}$	3	1/2	7/2	8/7	4.00	4.53

The concepts of the modulus of the moment ($\mathcal{m}_0$*) and the effective moment (*$\mathcal{m}_{eff}$*) were introduced in chapter 4, section 2.2.* La^{3+} *and* Lu^{3+}*, with their 4f shell being respectively empty and full, are non magnetic.*

This is immediately confirmed by noting that

$$J_x\,|a> = (3/2)\,|a> \quad \text{and} \quad J_x\,|b> = -(3/2)\,|b>,$$

which furthermore indicates that the eigenvalues of J_x are respectively $<J_x>_a = 3/2$, and $<J_x>_b = -3/2$.

Therefore the energies under the influence of the perturbation, i.e. in the magnetic field H_x, are

$$<E>_a = -8B_2^0 + <a|\,\mu_o H_x g_J \mu_B J_x\,|a> = -8B_2^0 + (3/2)\,\mu_o H_x g_J \mu_B, \text{ and}$$
$$<E>_b = -8B_2^0 + <b|\,\mu_o H_x g_J \mu_B J_x\,|b> = -8B_2^0 - (3/2)\,\mu_o H_x g_J \mu_B.$$

We conclude that the ground state, in the presence of the magnetic field along x, is $|b>$, and that its magnetic moment is $<m_x>_b = (3/2)\,g_J \mu_B$. Note that for a more accurate (but less pedagogical) treatment, it is necessary to consider the crystalline electric field, and Zeeman hamiltonians at the same order of perturbation. This involves diagonalising directly $\mathcal{H}_{cf} + \mathcal{H}_Z$ within the basis of the 2J + 1 states of the ground state multiplet.

EXERCISES

E.1 - Determine for the Sm^{2+} and Eu^{2+} ions, which have six and seven 4f electrons respectively, the values of S, L, J, g_J, and the maximum magnetic moment of the ground state.

E.2 - Iron, in its divalent and trivalent states, has $3d^6$ and $3d^5$ external configurations, respectively. Furthermore, these ions behave in many insulating materials as if their orbital moment was zero (by virtue of the crystal field). In this framework, determine, for Fe^{2+} and Fe^{3+}, the values of S, L, J, g_J, and the maximum magnetic moment of the ground state.

E.3 - The spin-orbit coupling coefficient, λ, of the Sm^{3+} and Tb^{3+} ions is –630 K and 580 K respectively. Give the values of S, L, J, g_J, and the maximum magnetic moment of the first excited multiplet for these ions. Also give, in kelvin, the energy difference between this, and the ground state.

E.4 - Let two identical charges q be located at $z = \pm a$ on the z axis. Write the expansion to second order in r / a of the potential $V(\mathbf{r})$ at a point M near the origin of a spherical co-ordinate system r, θ, φ. Deduce from this the second order term A_2^0 of the crystal field.

SOLUTIONS TO THE EXERCICES

S.1 Sm^{2+}: S = 3, L = 3, J = | L – S | = 0, $\mathfrak{m} = 0$.

Eu^{2+}: S = 7/2, L = 0, J = 7/2, $g_J = 2$, $\mathfrak{m} = 7\ \mu_B$.

S.2 Fe^{2+}: S = J = 3, $g_J = 2$, $\mathfrak{m} = 6\ \mu_B$. Fe^{3+}: S = J = 5/2, $g_J = 2$, $\mathfrak{m} = 5\ \mu_B$.

S.3 Sm^{3+}: S = 5/2, L = 5, J = | L – S | + 1 = 7/2, $g_J = 0.825$, $\mathfrak{m} = 2.89\ \mu_B$, $\Delta E = 2{,}205$ K.

Tb^{3+}: S = 3, L = 3, J = L + S – 1 = 5, $g_J = 3/2$, $\mathfrak{m} = 7.5\ \mu_B$, $\Delta E = 3{,}480$ K.

S.4 $A_2^0 = -\,|e|\,q / \varepsilon_0\, a^3\, \sqrt{5\pi}$ where |e| is the charge of an electron. Note that $A_2^0 < 0$ for $q > 0$, and vice versa.

REFERENCES

[1] C. COHEN-TANNOUDJI, B. DIU, F. LALOË, Quantum Mechanics (1992) Wiley & Sons; R.P. FEYNMAN, R.B. LEIGHTON, M. SANDS, The Feynman Lectures on Physics, Vol. 3 Quantum Mechanics (1964) Addison-Wesley; L.D. LANDAU, Quantum Mechanics (1997) Butterworth-Heinemann; H.J. ZEIGER, G.W. PRATT, Magnetic Interactions in Solids (1973) Clarendon Press, Oxford; J.C. SLATER, Quantum Theory of Atomic Structure, Vol. 1 (1960) McGraw-Hill Book Company.

[2] A. MESSIAH, Quantum Mechanics (2000) Dover.

[3] F.B. KOCH, M.E. FINE, *J. Appl. Phys.* **38** (1967) 1470.

[4] G. FOËX, C.J. GORTER, L.J. SMITS, Constantes sélectionnées diamagnétisme et paramagnétisme (1957) Masson & Cie dépositaires, Paris.

[5] K.H.J. BUSCHOW, *Rep. Prog. Phys.* **42** (1979) 1373.

[6] K.H.J. BUSCHOW, *Rep. Prog. Phys.* **40** (1977) 1179.

[7] M.T. HUTCHINGS, *in Solid State Physics* **16** (1964) 227, F. Seitz & D.T. Turnbull Eds, Acad. Press, New York.

[8] K.H.J. STEVENS, *Proc. Phys. Soc. London A* **65** (1952) 209.

[9] J.A. BLANCO, D. GIGNOUX, D. SCHMITT, *Phys. Rev. B* **45** (1992) 2529.

[10] D. SCHMITT, *J. Phys.* **47** (1986) 677.

In this alternative expression of Stoner's criterion, the quantity I is replaced by one that is more physical, viz the repulsion between two electrons on the same site. This is just as difficult to calculate in practice because the s electrons of the transition metals can shield the repulsion between d electrons. Therefore, it usually remains a parameter that is adjusted to fit experiment. It does show that the magnetism arises from a local repulsion, on a site, which will be useful in the following sections.

This analysis is at the origin of the theoretical model known as Hubbard's hamiltonian [5]. It allows the study of the effects of Coulomb repulsion, which was ignored in the simple independent electron theories. This model introduces a repulsion only for two electrons on the same site. They must therefore have opposite spins. The effects are not limited just to magnetism, but can explain why some compounds are insulators (so-called Mott insulators) whereas band theory would lead us to expect a metal [6].

6.3. CRYSTALLINE ELECTRIC FIELD

In metals and metallic compounds based on the transition metals, the elements lose their valence electrons as they form the conduction band. This leads to a network of positive charges in a sea of conduction electrons. We saw in section 6.1 that these electrons are not totally free: they are influenced by the periodic potential of the metallic ions in the lattice, and its symmetry. As in the localized electron model, the 3d electrons, on a given atom, are in the electric field produced by the charges of the surrounding ions, with a shielding effect from the other electrons. The spherical symmetry of the isolated ion is broken, and is replaced by the local symmetry of the lattice. The orbitals to be considered are no longer the eigenfunctions of the component to the angular momentum, but linear combinations of them.

For example, in a cubic environment, the d orbitals which were given by equations (7.29) will now be decomposed into orbitals that are generally termed e_g ($x^2 - y^2$, and $3z^2 - r^2$), and t_{2g} (xy, yz, and zx). While these orbitals have the same energy in a system with spherical symmetry, their degeneracy is broken in a cubic environment, as shown in figure 8.7. This splitting can be simply explained if we suppose that the first neighbors of the atom represented in the figure are positive charges situated on the axes Ox, Oy, and Oz; the e_g orbitals with their negatively charged electronic clouds point in the direction of these positive charges, which is energetically favorable, while the t_{2g} orbitals do not point towards the positive charges: this situation corresponds to a state of higher energy.

There is therefore a coupling between the orbitals and the lattice. This effect is referred to as the crystalline electric field or more simply crystalline field.

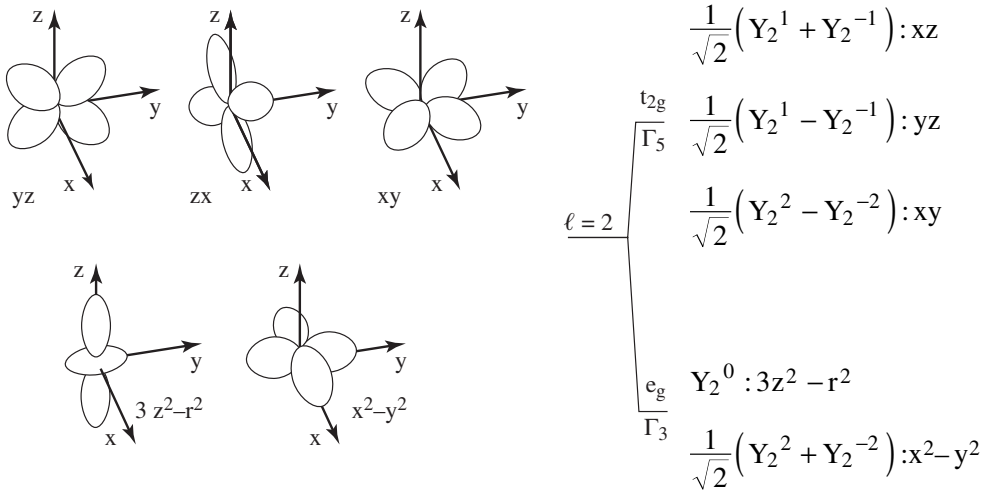

Figure 8.7 - Shapes of the d orbitals (on the left), and their splitting in a cubic environment (on the right)

In the tight binding approach, this effect is described by the integrals α (see § 5.1). In the transition metals, this effect is very small. However, in compounds such as the perovskites, the crystal field can lift the degeneracy completely. We show in figure 8.8 the example of a copper based perovskite, as is the case in the new superconducting materials. The symmetry of the perfect perovskite lattice is cubic. In the superconductors, a crystallographic distortion makes the structure tetragonal, and breaks the degeneracy of the e_g orbitals. The Fermi level in these materials is situated within the band formed from the $x^2 - y^2$ states.

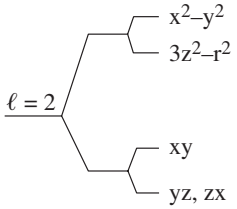

Figure 8.8 - Perovskites based on copper

6.4. MAGNETOCRYSTALLINE ANISOTROPY

The magnetocrystalline anisotropy depends both on the character of the orbitals at the Fermi level, and on the spin-orbit coupling. In metals, compounds, and alloys of transition metals, the spin-orbit coupling coefficient λ is always small compared to the crystal field parameters.

For the metals at the end of the first series, the crystal field is of the order of 1 eV, while the spin-orbit coupling, described in equation (7.20), is of the order of 0.01 eV. It can therefore be treated as a perturbation, and the anisotropy constants K_1, K_2, etc. can be determined from equations (3.3), and (3.4). One can shows that K_n decreases

289 K for Gd). This disparity is due to the variation in the magnitude of the magnetic moment with the different rare earths.

In chapter 20, section 4 we will show that the same long-range interactions are generally the origin of coupling between magnetic layers in multilayer systems. In these systems, it is possible to observe the oscillations in the RKKY exchange by varying the thickness of the non-magnetic layer which separates the two magnetic layers.

3.2. EXCHANGE INTERACTION IN THE 3d METALS

In chapter 8, we saw that, in the transition metals, the magnetic moment arises from a difference in the occupation of the bands with spin ↑ and ↓, and can therefore have non-integer values in terms of μ_B. This band-type magnetic moment appears when the intra-site Coulomb interaction, which tends to localize the electrons, is sufficiently large with respect to the kinetic energy of the d electrons. The interactions $U_{mm'}$ and $J_{mm'}$, previously defined (chap. 8), then lead to the stabilization of a localised magnetic moment on each site. This interaction between these moments takes place via overlap of the 3d wave functions of neighbouring sites (the transfer integrals β_{ij} defined in chap. 8). Notably, the s electrons, also present at the Fermi level, play a negligible role both in the stabilization of magnetic moments, and in the interaction between moments, as the polarization of the s band is negligible.

The overlap between wave functions has two contradictory effects: if $\beta >> U$ and J, the band will not be magnetic because Stoner's criterion will not be satisfied, and, if $\beta << U$ and J, the intersite exchange interactions will be weak. Figure 9.5 shows how the interactions vary as a function of U/β. The strongest interactions are obtained for values of U/β slightly greater than that corresponding to the onset of magnetism.

Figure 9.5 - Qualitative variation of the interactions between moments as a function of U/β

The critical value of $(U/\beta)_c$ corresponds to Stoner's criterion.

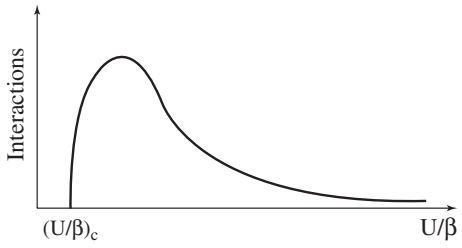

The sign of the interaction between 3d moments depends, as in the case of rare earths, on the filling of the band: it is ferromagnetic for a band that is nearly empty (or nearly full), and antiferromagnetic for a band that is half-filled.

It is possible to discuss very simply the sign of the exchange interaction for the transition metals. Consider two nearest-neighbor atoms with a small number of electrons (or holes). The ferromagnetic configuration will be preferred because it minimises the kinetic energy by permitting the electrons to delocalize from one atom to another (fig. 9.6), whilst still respecting Hund's rule. This is the situation in iron, cobalt, and nickel, where the 3d band is nearly full.

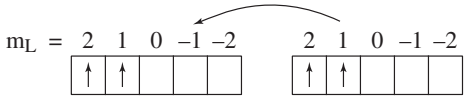

Figure 9.6 - Ferromagnetism in a nearly empty band

If the band is half-filled, the ferromagnetic configuration does not permit the electrons to be delocalized, as demonstrated in figure 9.7-a. However, the antiferromagnetic configuration does permit this, as shown in figure 9.7-b , and so it is the preferred configuration. This is the case for chromium and manganese. The antiferromagnetic structure in the first is sinusoidal, and in the second collinear.

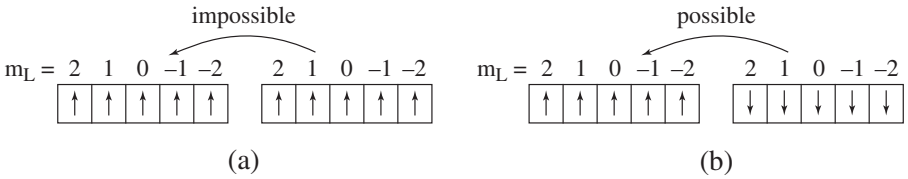

Figure 9.7 - Antiferromagnetism in a half-filled band

The value of the exchange between 3d magnetic moments depends strongly on the electronic structure. The Curie temperatures of iron and of cobalt are very high (respectively 1,043 and 1,388 K) but, in the compounds close to Stoner's instability, they are far lower, e.g. 6 K for Sc_3In.

3.3. DOUBLE EXCHANGE [7]

In the transition metal oxides, we have seen that the exchange interaction is of the superexchange type. This is only true for the interactions between ions that are in a definite valence state.

In certain oxides, the transition ion can feature two valence states depending on the doping: for example this is the case in the substitutional series $La_{1-x}Ca_xMnO_3$ or $La_{1-x}Sr_xMnO_3$, in which the fraction (1 – x) of Mn ions is in the configuration Mn^{3+} with a total spin S = 2, while the remainder of the Mn ions have the configuration Mn^{4+} (S = 3/2). Hybridization with the intermediate p orbitals of the O^{2-} ion in these manganites results in a ferromagnetic interaction between the Mn^{3+} and Mn^{4+} ions, called double exchange, as shown in figure 9.8. The ferromagnetic configuration (a) is stabilized by the reduction in the kinetic energy of the additional electron resulting from the delocalization associated with the hybridization.

Figure 9.8 - Following Hund's rule, the extra electron of the Mn^{3+} ion can delocalize onto the site of a neighbouring Mn^{4+} only if the spins are parallel [configuration (a)]. In the case of configuration (b), the extra electron remains localized on the Mn^{3+}

These same procedures can lead to the four state functions: $U(S, B_{//})$, $F(T, B_{//})$, $U(S, H)$ and $F(T, H)$. Their respective differentials are written:

$$dU(S, B_{//}) = TdS + \int HdB_{//}dV \tag{10.12}$$

$$dF(T, B_{//}) = -SdT + \int HdB_{//}dV \tag{10.13}$$

$$dU(S, H) = TdS - \int B_{//}dHdV \tag{10.14}$$

$$dF(T, H) = -SdT - \int B_{//}dHdV \tag{10.15}$$

3. *MAXWELL RELATIONS AND INEQUALITIES*

The eight functions defined above provide, via the Maxwell relations which generalise equation (10.4), physically useful expressions for the heat involved, or the variation in temperature, associated with the application of a magnetic field. Thus, the iso-entropic change in temperature can be described in terms of a magnetothermal coefficient, which can be deduced from equation (10.9) associated with $U(S, H_0)$:

$$\left(\frac{\partial T}{\partial H_0}\right)_S = -\mu_0\left(\frac{\partial m_{//}}{\partial S}\right)_{H_0} = -\mu_0\left(\frac{\partial m_{//}}{\partial T}\right)_{H_0}\left(\frac{\partial T}{\partial S}\right)_{H_0} = -\frac{\mu_0 T}{C_{H_0}}\left(\frac{\partial m_{//}}{\partial T}\right)_{H_0} \tag{10.16}$$

because $(\partial T/\partial S)_{H_0} = T/C_{H_0}$, where $C_{H_0} = T(\partial S/\partial T)_{H_0}$ is the heat capacity at constant applied field*. The determination of the finite change ΔT due to a finite change in applied magnetic field requires the use of an integration, and in the low-temperature regime it is definitely necessary to take into account the significant variation in C_{H_0} with magnetic field. This is in particular true for the most famous use of this technique: cooling by adiabatic suppression of the applied field, a technique (slightly improperly) called adiabatic demagnetization, which will be treated in an exercise at the end of chapter 11.

These relations lead to economy both in the concepts and in experiment. For example, relation (10.16) allows us to replace calorimetric measurements by isothermal magnetization measurements (see exercises).

In the same way that we have encountered, when dealing with the thermodynamics of simple systems, inequalities between the specific heats ($C_p > C_V$), we obtain inequalities between the coefficients that describe magnetic responses. In particular, $(\partial B/\partial H)_T$ and $(\partial B/\partial H)_S$, the isothermal and iso-entropic magnetic permeabilities $\mu_0\mu_{r_T}$ and $\mu_0\mu_{r_S}$ respectively, are always positive, with $\mu_{r_T} > \mu_{r_S}$.

If we also use this approach for the other pair of variables used, $\mathbf{H}_0$ and $\mathbf{M}$ or $\mathfrak{m}$, it appears to lead to the relation $(\partial M/\partial H_0)_{S \text{ or } T} > 0$. The fact that this relation is

---

* Not to be confused with the field coefficients of a coil (see Eq. 2.16).

2. THE MAGNETOCALORIC EFFECT

The reversible heating of para- or ferromagnetic substances which occurs during the ordering of the magnetic moments is known as the magnetocaloric effect. It is the inverse of the effect we just discussed: unlike an increase in temperature, an increase in the magnetic field strength reduces the disorder of the magnetic moments. If the magnetization process is performed in an adiabatic way, that is without heat exchange, the total entropy of the substance will remain constant: the ordering of the magnetic moments will be compensated for by a greater disorder in the atomic arrangement. This corresponds to an increase in temperature, *heating by adiabatic magnetization*.

Conversely, if a substance is magnetised at a given temperature, and then thermally isolated, the adiabatic demagnetization of this substance will cause its temperature to decrease: this is known as cooling by *adiabatic demagnetization*, and, in theory, allows the attainment of very low temperatures.

A simple description of this effect may be given in the framework of the molecular field theory. The variation in energy ΔE_{ex} which accompanies the application of a magnetic field H is again given by equation (11.2), but this time ΔM is the variation in magnetization created by H, and the work of the magnetic field H necessary to bring about this variation in magnetization is:

$$\Delta W = \mu_0 H \, \Delta M \tag{11.4}$$

The heat which is produced by this process will be equal to the difference between the work done by the field and the variation in exchange energy:

$$\Delta Q = \mu_0 (H + w M) \, \Delta M \tag{11.5}$$

where $w M$ is the molecular field. For temperatures *above the Curie temperature,* equations (4.50) and (4.51) allow us to write the molecular field as:

$$wM = H T_C / (T - T_C) \tag{11.6}$$

which finally gives us the heat generated by magnetization reversal in the paramagnetic regime:

$$\Delta Q = \frac{1}{2} \frac{\mu_0}{w} \frac{T \, T_C}{(T - T_C)^2} \Delta(H^2) \tag{11.7}$$

This generated heat will therefore raise the temperature of the sample by a proportional quantity, $\Delta T = \Delta Q / C_M$. This is the magnetocaloric effect. C_M is the specific heat at constant magnetization, and T is the initial temperature of the sample, in the absence of a magnetic field. Indeed, P. Weiss and R. Forrer observed, and precisely measured this heating in nickel; some of their results are reproduced in figure 11.2, which clearly shows that, above T_C, the heating varies as the square of the magnetic field, and decreases rapidly with temperature.

where j is the current density in the wire and $H_{//}$ is the magnetic field applied along the axis of the sample, *provided the magnetic field due to j remains small with respect to $H_{//}$.*

Figure 12.26 shows the elegant experiment performed in 1919 by Pidgeon on an annealed nicked wire, 1 mm in diameter, submitted to a magnetic field $H_{//} = 22.3\ kA.m^{-1}$.

The twist is described by equation $\xi = -6.74\times10^{-5} - 2.40\times10^{-9} j\ (rad.m^{-1})$ if the current density j is expressed in $A.m^{-2}$. This yields for the magnetostriction coefficient λ_s the value -35.7×10^{-6}, in excellent agreement with the most recent results ($\lambda_s = -36\times10^{-6}$). This effect was also used to determine the magnetostriction coefficient for amorphous metallic ribbons: formula (12.31) also applies in this case.

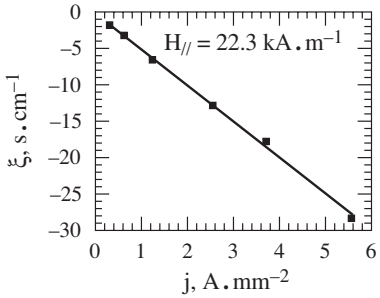

Figure 12.26 - Wiedemann effect for a nickel wire [19]

The twist ξ, expressed in arcseconds per centimetre, varies linearly with the current density.

6. INVERSE MAGNETOELASTIC EFFECTS AND THE ΔE EFFECT

After describing the direct magnetoelastic effects, we now show how the magnetic properties of a material can be altered through the application of mechanical stresses.

6.1. EFFECT OF HYDROSTATIC PRESSURE ON A MAGNETIC MATERIAL

Hydrostatic pressure is isotropic, hence it cannot lower the symmetry of a material. It will therefore change only the value of the Curie temperature and of the magnetic moment. Since the latter can be anisotropic in a material with uniaxial symmetry, the variation in moment under hydrostatic pressure can be different along the c axis and in the basal plane for such materials.

The variations in Curie temperature under pressure are usually small, except for materials featuring the Invar effect ($\partial T_C / \partial P = -35\ K.GPa^{-1}$ for $Fe_{64}Ni_{36}$ and $-24\ K.GPa^{-1}$ for the amorphous alloy $Fe_{80}B_{20}$) [20]. There exist fewer data on the pressure variations of magnetic moments, because these are difficult measurements.

Thermodynamic relations have been established between forced magnetostriction, the pressure variation of magnetic moment, and the pressure variation of T_C as expressed by the logarithmic derivative $\Gamma = \partial\ln(T_C)/\partial\ln(V)$. Thus [17]:

$$\mu_0 (\partial \mathfrak{m} / \partial p) = -(\partial V / \partial H) = -V (\partial \lambda^{\alpha,0} / \partial H) \tag{12.32}$$

$$\frac{\partial \lambda^{\alpha,0}}{\partial H}(T) = \frac{m \dfrac{\partial \lambda^{\alpha,0}}{\partial H}(0) - 3 \dfrac{\mu_0 T}{c^\alpha V} \left(\dfrac{\partial \mathfrak{m}}{\partial T} \right)_p \Gamma}{1 - 3\alpha_T T \Gamma} \tag{12.33}$$

where $m = M(T)/M(0)$ is the reduced magnetization at temperature T, and $\mathfrak{m}$ the magnetic moment associated to volume V of magnetised material; c^α is $c_{11} + 2\,c_{12}$ and α_T is the linear thermal expansion coefficient. The first relation shows that forced volume magnetostriction is proportional to the pressure variation of magnetic moment. The second relation shows that it features a maximum around T_C (where $\partial \mathfrak{m}/\partial T$ becomes strongly negative), this maximum being the sharper the larger is Γ: Γ is less than one in most materials, it is 5 for the amorphous alloy $Fe_{80}B_{20}$ and 17 for the crystallised alloy $Fe_{64}Ni_{36}$ (Invar®).

6.2. *EFFECT OF A UNIAXIAL STRESS ON THE MAGNETIZATION CURVE*

We now discuss an essential effect, which has a strong influence on the performance of magnetic materials and has often been used to make sensors. A uniaxial stress deforms the material and this generates a magnetic anisotropy proportional to the strain and alters the magnetic permeability. Understanding the mechanism of this stress-induced anisotropy is essential for mastering its effects.

6.2.1. *Material with cubic symmetry*

The anisotropic part of the magnetoelastic coupling energy (12.10) can be rewritten, taking (12.16) into account, in the form:

$$E_{mel} = -\lambda^{\gamma,2}\sigma\left[\frac{2}{3}\left(\alpha_3{}^2 - \frac{\alpha_1{}^2 + \alpha_2{}^2}{2}\right)\left(\gamma_3{}^2 - \frac{\gamma_1{}^2 + \gamma_2{}^2}{2}\right) + \frac{1}{2}\left(\alpha_1{}^2 - \alpha_2{}^2\right)\left(\gamma_1{}^2 - \gamma_2{}^2\right)\right]$$
$$- 2\,\lambda^{\varepsilon,2} c^\varepsilon (\varepsilon_{yz}\alpha_2\alpha_3 + \varepsilon_{zx}\alpha_3\alpha_1 + \varepsilon_{xy}\alpha_1\alpha_2) \tag{12.34}$$

We saw in section 3 that the formalism used here diagonalises Hooke's law, which results in a linear relationship between stress (σ) and strain (ε):

$$c^\gamma\left(\varepsilon_{zz} - \frac{\varepsilon_{xx} + \varepsilon_{yy}}{2}\right) = \sigma_{zz} - \frac{\sigma_{xx} + \sigma_{yy}}{2}$$
$$c^\gamma(\varepsilon_{xx} - \varepsilon_{yy}) = (\sigma_{xx} - \sigma_{yy}) \tag{12.35}$$
$$c^\varepsilon \varepsilon_{yz} = \sigma_{yz} \quad c^\varepsilon \varepsilon_{zx} = \sigma_{zx} \quad c^\varepsilon \varepsilon_{xy} = \sigma_{xy}$$

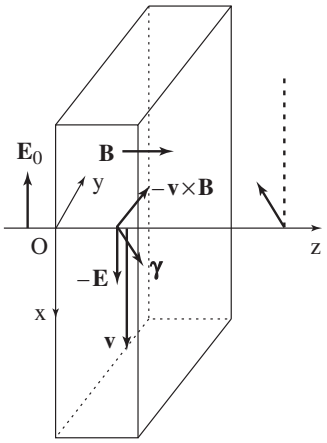

Figure 13.5 - Schematic representation of the Kerr effect in a classical approach

This shows the effect of a thin slab of magnetic material. The contributions $-e\,\boldsymbol{E}$ and $-e\,\boldsymbol{v}\times\boldsymbol{B}$ to the acceleration of the electrons would lead to a resulting acceleration $\boldsymbol{\gamma}$ that is not colinear to $\boldsymbol{E}$. The contribution from this slice to the wave radiated at large distance will therefore not be colinear to $\boldsymbol{E}$ either. This figure does not include the effect of the propagation time.

Thus the radiated wave will not be polarised along the x direction. In other words, rectilinear polarization along x or y is not an eigenmode for propagation in the material in the presence of **B**. Formal analysis shows that the eigenmodes which propagate without being altered in the material in the presence of **B** are the left- and right-hand circular polarizations L and R. Well-defined refractive indices, n_L and n_R, are associated with these eigenmodes.

When absorption is taken into account, the refractive index for the material and ε both are complex, even in the absence of magnetic field. The same is true for the non-diagonal terms of the permittivity tensor in the presence of **B**.

These are the two ingredients of the *Faraday effect*. The difference between the imaginary parts of the non-diagonal terms in **ϵ'** leads to the right-hand component E_R and the left-hand component E_L having a phase difference $2\pi\, d\,(n_L - n_R)/\lambda_0$, after travelling the same distance d, with λ_0 the wavelength in vacuum (circular birefringence). Their sum **E'** will thus, in the absence of absorption, be a rectilinear vibration rotated by an angle θ_F proportional to d (fig. 13.6).

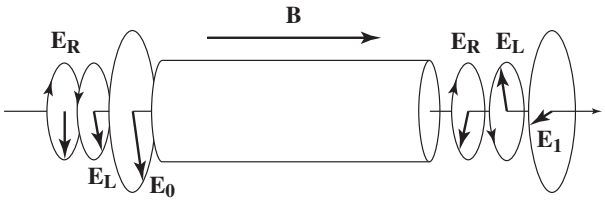

Figure 13.6 - The rotation associated with the Faraday effect is due to the difference in velocity of the right-hand E_R vibration and left-hand vibration E_L, hence of the indices n_R and n_L

The electric field vectors are shown before ($\boldsymbol{E}_0$) and after ($\boldsymbol{E}_1$) going through the magnetic sample. The arrows $\boldsymbol{E}_R$ and $\boldsymbol{E}_L$ in each group correspond to the same point and the same time, and the amplitudes of $\boldsymbol{E}_R$ and $\boldsymbol{E}_L$ correspond to their superposition, at the same points. Rotation of the polarization of light is due to the velocity for $\boldsymbol{E}_L$ being larger.

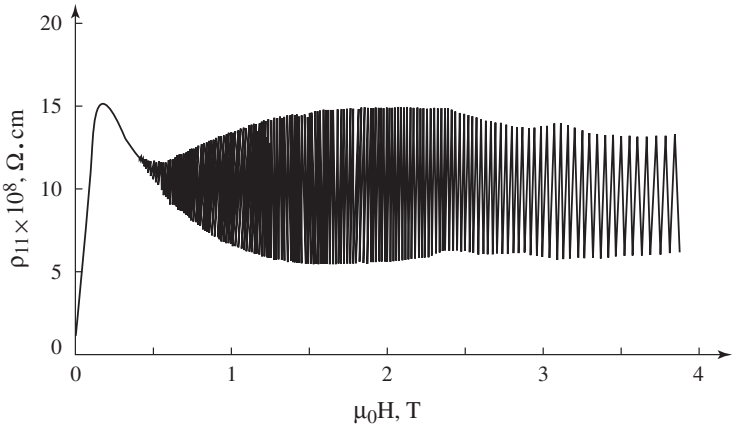

Figure 14.11 - Shubnikov-de Haas effect in Mg, from ref. [36]

5.2. THE QUANTUM HALL EFFECT

This effect (QHE) was discovered in 1980 by K. von Klitzing *et al.* [37]. It appears at very low temperatures for a layer of electrons confined to two dimensions (at the junction between two semiconductors). Unlike the preceding case, there is no z degree of freedom ($k_z = 0$ in eq. 14.13). In contrast to the classical Hall effect, the Hall voltage increases in steps as a function of field; these steps correspond to a reduction or even cancellation of the longitudinal resistivity [35, 38]. Each plateau of the Hall conductance corresponds to a multiple (integral QHE) or sub-multiple (fractional QHE) of the *conductance quantum* e^2/h, independently of the nature of the sample under consideration: $\rho_H = h/\nu e^2$. The values of the resistance plateaus are the same, to better than 10^{-7}, as the calculated theoretical values. This has allowed a new standard of resistance to be defined: the ratio (h/e^2), or the klitzing, is 25,812.8 ohms.

What do these steps correspond to? The Hall resistivity represents the ratio of the field to the electronic density: $\rho_H = B/ne$. The flux in the sample being a multiple of the elementary flux quantum Φ_0, the steps appear for definite values, integral or fractional, of the *filling factor*, the ratio between the number of electrons and the number of flux quanta. The integral QHE corresponds to the occupation of an integral number of Landau levels. The existence of a *gap* in the excitation spectrum makes the electron gas incompressible. More generally, the repulsive interactions between electrons stabilise a new type of quantum fluid, where the electrons are linked to the flux quanta. The phenomenon can thus be interpreted as a condensation of fermions, under the influence of an intense field, into bosons subjected to a reduced field [39]. This condensation into bosons explains the cancellation of the longitudinal resistance, and has analogies with superconductivity.